Electrochemical study of the Cu^{2+} sensor based on ZIF-67/MWCNTs/Nafion

Lifeng Ding , Yuru Song , Qiang Li * , Qi Wang , Jie Zhang , Zhengwei Song , Shengling Li , Jiayu Liu , Xin Zhang

Posted Date: 2 January 2024

doi: 10.20944/preprints202401.0076.v1

Keywords: Metal Organic Framework; Nanocomposite; Detection of heavy metal Cu^{2+}; Electrochemical Sensor

Article

Electrochemical Study of the Cu^{2+} Sensor Based on ZIF-67/MWCNTs/Nafion

Lifeng Ding [1,2,†], Yuru Song [1,2,†], Qiang Li [3,*], Qi Wang [1], Jie Zhang [1], Zhengwei Song [1], Shengling Li [1], Jiayu Liu [1] and Xin Zhang [1]

[1] Department of Chemistry and Chemical Engineering, Taiyuan Institute of Technology, Taiyuan 030008, PR China
[2] School of Chemical Engineering and Technology, North University of China, Taiyuan 030051, PR China
[3] MicroNano System Research Center, College of Information and Computer & Key Laboratory of Advanced Transducers and Intelligent Control System of Ministry of Education and Shanxi Province, Taiyuan University of Technology, Taiyuan, 030024, PR China
* Correspondence: liqiang02@tyut.edu.cn
† These authors contributed equally to this work.

Abstract: In this work, a ZIF-67/MWCNTs/Nafion sensor platform was constructed based on the good adsorption capacity of ZIF-67, the electrical conductivity of multiwalled carbon nanotubes (MWCNTs) and the excellent chemical stability of Nafion for the detection of Cu^{2+} in water. Meanwhile, the modified materials were characterized by scanning electron microscopy (SEM), Transmission electron microscopy (TEM), BET specific surface area test, X-ray photoelectron spectroscopy (XPS), X-ray diffraction (XRD) and Fourier transform infrared spectrometry (FT-IR). Cyclic voltammetry (CV), electrochemical impedance (EIS), and square wave solvation voltammetry (SWSV) electrochemical methods were used to perform applied test studies on ZIF-67/MWCNTs/Nafion/GCE. The results show that ZIF-67/MWCNTs/Nafion/GCE has high sensitivity (57.5 μA/μM) and a low limit of detection (15.0 nM) for the electrochemical detection of Cu^{2+} ions in an electrochemical sensing system. It has high adsorption selectivity for Cu^{2+}, and the recovery of Cu^{2+} in real water reached 98.6%-103%. The modified electrode has good repeatability, reproducibility, anti-interference, and stability, which makes this sensing platform can be practically applied to the detection of domestic water.

Keywords: metal organic framework; nanocomposite; detection of heavy metal Cu^{2+};·electrochemical sensor

1. Introduction

Heavy metals are highly toxic and difficult to be degrade, posing a serious threat to the environment and human health [1]. Although copper ions are an essential trace element of the human body, excessive participation will cause damage to human function. Therefore, it is particularly critical to find an efficient, fast and sensitive method to detect the content of copper ions in a precise way. To date, various analytical and detection technologies have been used for the detection of heavy metals, such as high-performance liquid chromatography (HPLC) [2], inductively coupled plasma−mass spectrometry (ICP−MS) [2] and UV−visible spectroscopy (UV−Vis) [3], while the disadvantages of large equipment, high price, and complex operation limit their practical application. Compared with traditional detection methods, electrochemical sensors have the advantages of high sensitivity, good selectivity, rapid detection, low price and easy operation [4,5]. However, bare electrode detection has problems such as low selectivity and repeatability. How to further select the electrode modification materials and construct an electrochemical sensing platform to improve the detection performance of heavy metal ions is still a challenge in electrochemical sensor research. Therefore, exploring a high-performance electrode modification material plays an important role in the preparation of electrochemical sensors.

Preprints (www.preprints.org) | NOT PEER-REVIEWED | Posted: 2 January 2024 doi:10.20944/preprints202401.0076.v1

Metal organic framework (MOF) materials are coordination polymers composed of metal units and organic linkers [6]. It is considered as an ideal material for electrode modification due to its large surface area, uniform distribution of pores and good adsorption properties. The cobalt-based imidazolate zeolite skeleton (ZIF-67) with rhombic dodecahedral structure is widely used in the field of sensors for food analysis [7,8], biomedicine[9,10], and environmental monitoring [11–13] due to its good adsorption capacity. Therefore, ZIF-67 was selected as an electrode modification material to construct an electrochemical sensing platform for detecting heavy metal ions. Unfortunately, the low conductivity and poor stability of the material in aqueous solution seriously hinder its application in electrochemical sensors. To solve the abovementioned problem of the ZIF-67 electrode, postsynthetic modification methods [14–16] were used to enhance the electrochemical activity and conductivity of pure ZIF-67 [17].

Multiwalled carbon nanotubes (MWCNTs) have a more efficient detection area and faster electron transfer rate than ordinary electrode-modified materials due to their unique tubular structure [18,19] and have been deemed potential materials to modify ZIF-67. At the same time, Nafion is the most commonly used ion exchange polymer in the determination of heavy metals. It has important properties such as chemical inertia, nonelectroactivity, hydrophilicity, and insolubility in water [20] and has been widely used for electrode surface modification [21,22]. In addition, Nafion can not only effectively adsorb heavy metal ions but also be used as a modifier to firmly attach the modified material to the electrode surface, thus improving its stability. Thus, Nafion was used to improve the stability of the ZIF-67/MWCNTs-modified layer to obtain the final composite material (ZIF-67/MWCNTs/Nafion) to detect Cu^{2+} ions in an electrochemical sensing system. Cu^{2+} detection by ZIF-67/MWCNTs/Nafion/GCE as a sensing platform has not been reported.

Based on the above analysis, in this work we introduced MWCNTs into ZIF-67 to synthesize ZIF-67/MWCNTs/Nafion composites, dedicated to the efficient detection of Cu^{2+} in domestic water (Scheme 1). The effects of pH, deposition time, deposition potential, interfering ions, and Cu^{2+} concentration on with the detection of Cu^{2+} were investigated. The kinetic and isotherm characteristics of Cu^{2+} adsorption by ZIF-67/MWCNTs/Nafion and the adsorption mechanism were investigated. This work is expected to provide an effective strategy for the rational modification of MOF-based adsorbents for effective application in the detection of Cu^{2+} in domestic water.

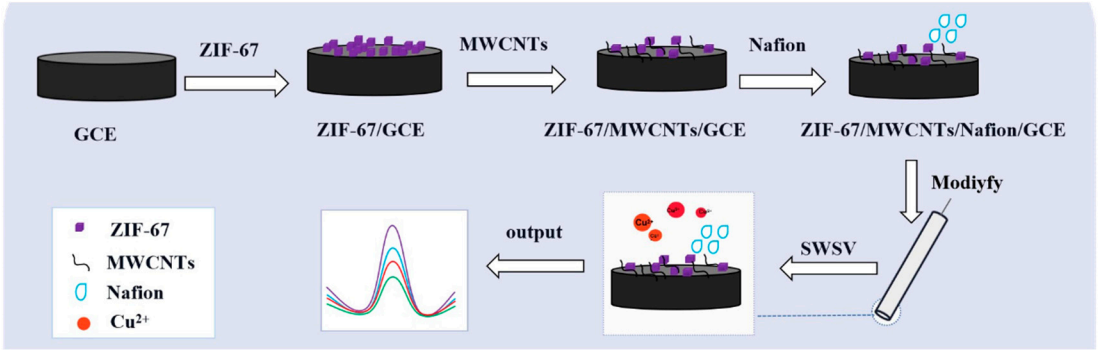

Scheme 1. Schematic diagram of the preparation process of the ZIF-67/MWCNTs/Nafion/GCE electrochemical sensor for the sensitive detection of Cu^{2+}.

2. Experiment

2.1. Chemical reagents

2-Methylimidazole (2-MI, 98%) and Cobalt nitrate hexahydrate ($Co(NO_3)_2{\cdot}6H_2O$, 99%) were obtained from Shanghai Macklin Technology Co., Ltd. Sodium hydroxide (NaOH, AR), Methanol (CH_3OH, AR) and Potassium ferrocyanide ($K_3[Fe(CN)_6]$, AR) were obtained from Tianjin Tianli Chemical Reagent Co., Ltd. Multiwalled carbon nanotube (MWCNTs, 97%) was obtained from Kaisa New Materials Co., Ltd. Nafion (5%, AR) was purchased from Shanghai Hesen Electric Co., Ltd. Ammonia ($NH_3 \cdot H_2O$, AR) and Acetic acid (HAc, AR) were supplied by Xilong Chemical Co., Ltd.

 doi:10.20944/preprints202401.0076.v1

Sodium acetate (NaAc, AR) was purchased from Tianjin Beichen Fangzheng Reagent Factory. Ammonium chloride (NH_4Cl, AR) was obtained from Tianjin Shentai Chemical Reagent Co., Ltd. Potassium chloride (KCl, AR) was supplied by Tianjin Guangfu Technology Co., Ltd. The solutions in the experiments were all obtained from deionized water (18.2 MΩ·cm) as the water source, which was purified by the UPC system. Real water samples were selected for testing from the tap water of Taiyuan Institute of Technology, Jiancaoping District, Taiyuan City, and mineral water from Cestbon. All materials and reagents are non-toxic and harmless. Additionally, all the materials and chemicals were used as received directly from the suppliers without any further treatment.

2.2. Preparation of ZIF-67

According to previous reports, the synthesis steps of ZIF-67 are as follows [23] : First, 1.17 g $Co(NO_3)_2{\cdot}6H_2O$ and 1.4 g 2-MI were weighed with an electronic balance and added into 50 mL of CH_3OH, respectively. After stirring with a glass rod to clarify, the two were mixed immediately and stirred in a magnetic stirrer for 30 min. Second, the mixed solution was centrifuged at a rotational speed of 8000 r/min. Finally, the centrifuged product was dried at 60°C for 12 h and ground to obtain ZIF-67.

2.3. Purification Treatment of MWCNTs

Purification of MWCNTs can improve the agglomeration of MWCNTs by increasing the content of oxygen-containing functional groups such as hydroxyl and carboxyl groups [24]. The steps are as follows: MWCNTs were put into 20 mL $V(H_2SO_4)$:$V(HNO_3)$= 1:3 mixed acid at 40°C continuous reflux for 6 h, and then washed with water to neutral. Finally, the product was dried in an oven.

2.4. Fabrication of ZIF-67/GCE, ZIF-67/MWCNTs/GCE, ZIF-67/MWCNTs/Nafion/GCE

ZIF-67 (1 mg/mL) and MWCNTs (0.5 mg/mL) were ultrasonicated for 5 min to obtain a uniform dispersion solution. Nafion (5%) was diluted with methanol. Before modifying the electrode, the working electrode was polished by Al_2O_3 and cleaned by ultrasonication. After drying, ZIF-67, ZIF-67/MWCNTs, and ZIF-67/MWCNTs/Nafion modification solutions were applied in drops and dried under a red lamp to obtain the corresponding electrode.

2.5. Instruments and measurements

The morphology and microstructure of the modified materials ZIF-67 and MWCNTs were characterized by scanning electron microscopy (SEM, HITACHI SU8010) and transmission electron microscopy (TEM, FEI Tecnai G2F30). The crystal structure of the modified materials ZIF-67 and MWCNTs were examined by X-ray diffraction (XRD, Bruker D8 Advance). The functional groups contained in MWCNTs before and after the modification treatment were characterized by Fourier transform infrared spectroscopy (FT-IR, Nicolet lS10); The N_2 adsorption-desorption (BET, Micromeritics ASAP 3020) technique was used to determine the surface area and pore structure of the modified materials ZIF-67, ZIF-67/MWCNTs. X-ray photoelectron spectroscopy (XPS, Thermo Escalab 250XI) was used to examine the elemental composition and valence of ZIF-67.

All electrochemical experiments in this work were carried out at Princeton ParSTAT MC multichannel electrochemical workstation. A glassy carbon electrode (L-type, 3 mm) was used as the working electrode, a saturated Ag/AgCl electrode as the reference electrode, and a platinum sheet electrode as the counter electrode. The electrolyte was 0.1 M HAc-NaAc buffer solution (pH=5.0). The pH of the HAc-NaAc buffer was adjusted with 0.1 M HCl and 0.1 M NaOH. Square wave dissolution voltammetric curves were measured at a deposition potential of -0.4 V, a deposition time of 150 s, and a measurement range of -0.4~0.6 V. Cyclic voltammetry (CV) and electrochemical impedance (EIS) measurements were carried out in $K_3[Fe(CN)_6]$ solution in 1 M KCl. Cyclic voltammetric curves were measured in the potential range of -0.2 V ~ 0.8 V with a scan rate of 20 mV/s. EIS was performed in the frequency range of 100,000 ~ 0.1 Hz.

Preprints (www.preprints.org) | NOT PEER-REVIEWED | Posted: 2 January 2024 doi:10.20944/preprints202401.0076.v1

3. Results and discussion

3.1. Characterization of electrode modification materials

The structures of ZIF-67 and MWCNTs were analyzed by XRD, and the physical and chemical properties of the materials were determined. The XRD pattern of ZIF-67 (Figure 1a) shows that the diffraction peak is basically consistent with that of simulated ZIF-67, which proves that ZIF-67 has been successfully synthesized [25]. The diffraction peaks of the acidified MWCNTs (Figure 1b) at 26.35° and 44.12° corresponded to the characteristic peaks of graphic-carbon standard card PDF#75-1612, indicating that the skeleton was intact and intact after acid treatment [26].

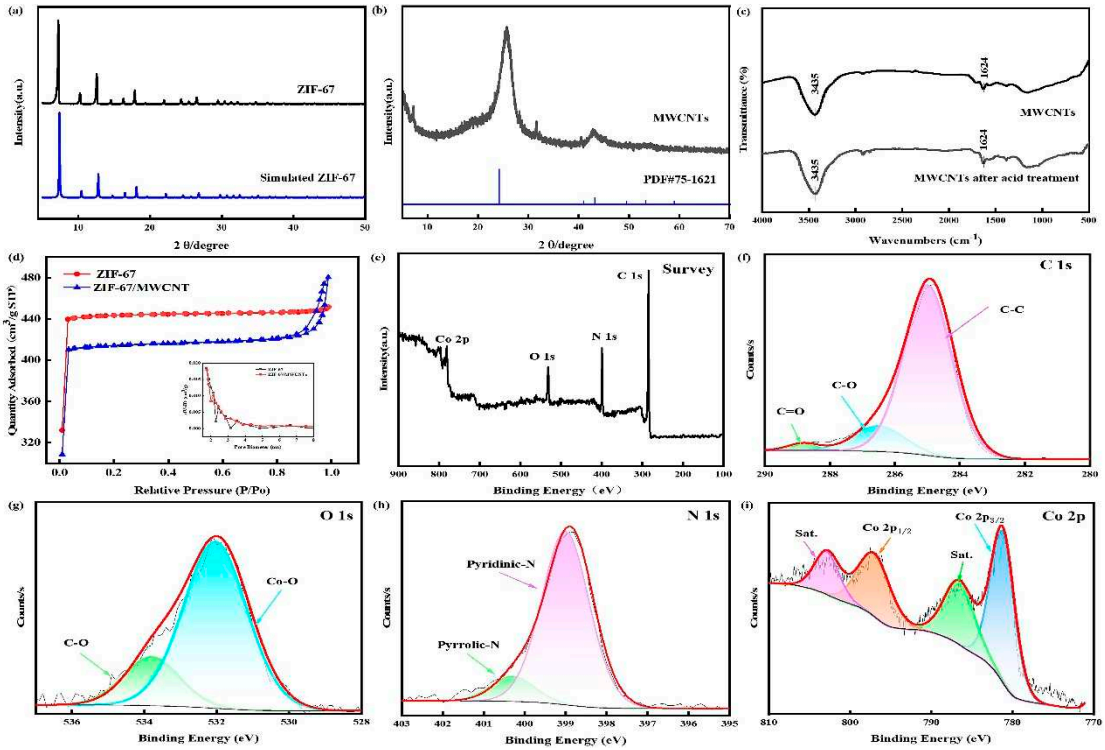

Figure 1. XRD patterns of (a) ZIF-67 (b) MWCNTs; (c) FTIR spectra of MWCNTs before and after acid treatment; (d) N2 sorption isotherms of ZIF-67 and ZIF-67/MWCNTs (inset shows the corresponding pore size distribution curves distribution curves); (e) Full XPS spectrum of ZIF-67, High resolution XPS spectrogram of (f) C 1s (g) O 1s (h) N1s (i) Co2p.

FTIR plays an important role in identifying functional groups. Figure 1c is the FTIR spectrum of MWCNTs before and after acidification treatment. The absorption peak caused by the C=O stretching vibration in -COOH appeared at 1624 cm^{-1} [27], and the stretching vibration peak of -OH caused by intramolecular association appeared at 3435 cm^{-1} [28,29]. This result shows that there are a certain amount of -OH and -COOH functional groups in the MWCNTs. The absorption peak of acid-treated MWCNTs was sharper at 1624 cm^{-1}, indicating that the mixed acid introduced more C=O to the MWCNTs. At the same time, C=O was further oxidized into -COOH, which increased the carboxyl functional groups. The absorption peak at 3435 cm^{-1} widened, indicating that acidification introduced more -OH into the surface. In conclusion, acid treatment increases the amount of carboxyl and hydroxyl groups on the surface of MWCNTs, which greatly improves the dispersity of MWCNTs.

Specific surface area and pore size distribution are important parameters affecting the performance of electrode materials. Thus, the N_2 adsorption-desorption isotherms and pore size distributions of ZIF-67 and ZIF-67/MWCNTs were investigated. As shown in Figure 1d, both ZIF-67 and ZIF- 67/MWCNTs exhibited type I isotherms. The average pore size was 4.8478 nm, which was in the range of 2-50 nm, indicating that the pores were mainly composed of mesopores.The BET specific surface area (SBET) of the ZIF-67 and ZIF-67/MWCNTs nanocomposites were 1324.1918 m^2/g

 doi:10.20944/preprints202401.0076.v1

and 1237.6814 m^2/g, respectively.The prepared ZIF-67/MWCNTs had relatively low specific surface area, which may be due to the fact that MWCNTs occupy a part of the pore volume of ZIF-67 in their attachment to ZIF-67. Overall, the ZIF-67/MWCNTs exhibited a large specific surface area, which is expected to play a positive role for the adsorption and conductivity properties of Cu^{2+}.

The element types and chemical states in the sample ZIF-67 were analyzed by XPS. Figure 1e is the full XPS spectrum of ZIF-67, which confirms that C, O, N and Co coexist in ZIF-67. Peaks of C1s, O1s, N1s and Co 2p are clear without obvious impurity peaks. The results are in good agreement with the XRD and SEM test results, which proves that the material has been successfully synthesized. The C1s spectrum of ZIF-67 (Figure 1f) show that there are mainly three different types of C in C1s, which are C-C (284.7 eV), C-O (286.4 eV) and C=O (288.8 eV). Meanwhile, the O1s spectrum (Figure 1g) corresponds to the Co-O bond and C-O bond at 532.1 eV and 533.7 eV, respectively. The N1s XPS spectrum shows that the peaks at 398.6 eV and 400.2 eV, respectively, correspond to two states of nitrogen existence in the material: pyridine-N and pyrrorole-N [30–32] (Figure 1h). According to the XPS spectrum of Co 2p, the peaks at 796.7 eV and 781.2 eV are characteristic peaks of Co $2p_{1/2}$ and Co $2p_{3/2}$, respectively [33,34] (Figure 1i). In addition, there are two satellite peaks, 802.1 eV and 786.2 eV, which confirm the presence of Co^{2+} in ZIF-67 [35,36]. This indicates that cobalt in ZIF-67 exists in the form of divalent ions.

The morphology of the electrode modification solution after sonication was characterized using scanning electron microscopy (SEM) and transmission electron microscopy (TEM). As shown in Figure 2a,b, the skeleton structure of ZIF-67 is intact, uniform in shape and clearly visible in outline. It has a typical and regular rhomboidal dodecahedron structure, part of which is broken into fine particles under the action of ultrasound. As shown in Figure 2c,d, the acidified MWCNTs showed a tubular structure, uniform diameter, smooth surface, and well-ordered dispersion. From the TEM results (Figure 2g,h), it was further demonstrated that the MWCNTs after acidification were in a hollow tubular structure, which provided conditions for Cu^{2+} transport. The modification liquid after ultrasonic mixing of ZIF-67 and MWCNTs in a certain proportion is shown in Figure 2e,f. ZIF-67 was completely broken into nanoparticles and wrapped together with tubular MWCNTs.

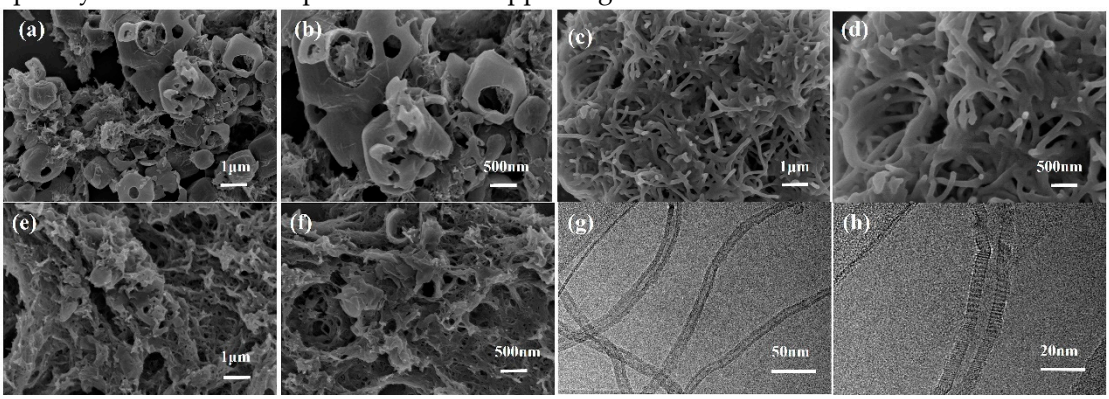

Figure 2. SEM images of (a) and (b) ZIF-67, (c) and (d) MWCNTs, (e) and (f) ZIF-67/MWCNTs at different magnifications after ultrasound; TEM images of (g) and (h) MWCNTs at different magnifications after ultrasound.

3.2. Electrochemical characterization of electrodes

The electrochemical properties of the GCE, ZIF-67/GCE, MWCNTs/GCE and ZIF-67/MWCNTs/GCE were tested by CV and EIS in a 5 mM $K_3[Fe(CN)_6]$ solution containing 1 M KCl. Figure 3a shows the CV curves of different modified materials with a scanning range of -0.2V to 0.8 V and a scanning rate of 20 mV/s. After comparison of the four electrodes, it was found that MWCNTs/GCE showed the highest peak current and the lowest peak potential difference (the difference between the oxidation peak and the reduction peak, 57 mV), which can be attributed to the peak potential difference being inversely proportional to the electron transfer rate constant [37]. MWCNTs have the highest electron transfer rate constant among the four, indicating the good electrical conductivity of MWCNTs. Compared with ZIF-67/GCE, the oxidation peak current of ZIF-

Preprints (www.preprints.org) | NOT PEER-REVIEWED | Posted: 2 January 2024 doi:10.20944/preprints202401.0076.v1

67/MWCNTs/GCE increased by approximately 37%, while the peak potential difference decreased from 110 mV to 90 mV, indicating that the addition of MWCNTs improved the conductivity of ZIF-67. In order to investigate the charge transfer resistance between the electrode modification material and the electrolyte interface, electrochemical impedance spectroscopy (EIS) test method was used. The solution resistance (Rs) denotes the intersection of the semicircle in the high frequency region with the x-axis. The charge transfer resistance (Rct) indicates the charge transfer rate, and the size is the diameter of the semicircle [38]. The smaller the diameter of the semicircular arc, the smaller the resistance to electron transfer, the faster the rate of electron movement, and the better the conductivity of the material modified on the electrode surface. From the Nyquist plot in Figure 3b, it can be seen that the diameter of the semicircular arc of MWCNTs/GCE is the smallest, indicating that MWCNTs have the best electrical conductivity. Compared with ZIF-67/GCE, ZIF-67/MWCNTs/GCE showed a smaller semicircle diameter and a correspondingly smaller electron transport resistance, indicating that MWCNTs improved the conductivity of ZIF-67, which was consistent with the CV results.

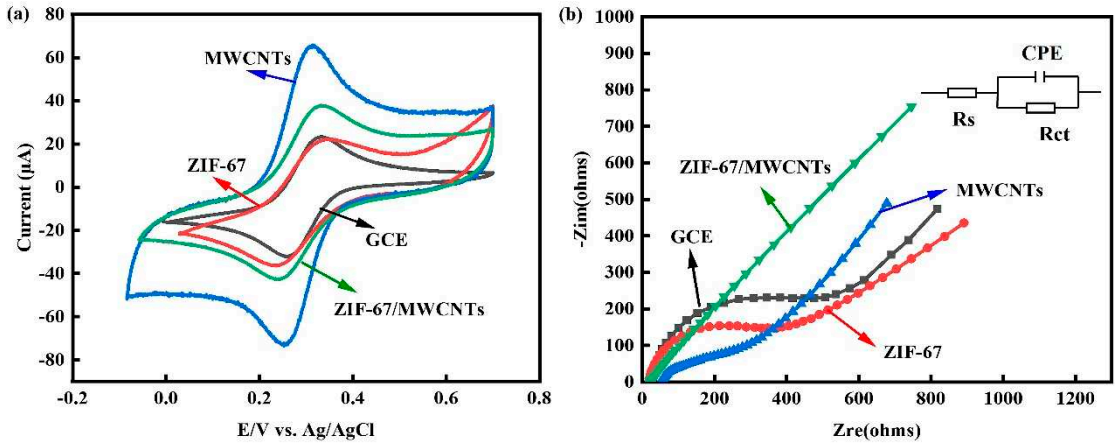

Figure 3. a) CV and (b) EIS of bare GCE, ZIF-67/GCE, MWCNTs/GCE , ZIF-67/MWCNTs/GCE.

3.3. Optimization of test conditions

Through the above studies, ZIF-67/MWCNTs/Nafion/GCE was used as the electrochemical sensor for the detection of Cu^{2+}. To obtain the best sensing performance, the key experimental parameters were optimized. The Optimization parameters are as follows: type of electrolyte solution, pH of electrolyte solution, deposition time and deposition potential (Figure 4). In short, the following experimental conditions were found to have the best results: (a) 0.1 M HAc-NaAc electrolyte solution with pH 5; (b) The deposition potential was -0.4 V, and the deposition time was 150 s, taking into account factors such as modification material, electrode loss and test efficiency. The following experiments were carried out under the above conditions.

Preprints (www.preprints.org) | NOT PEER-REVIEWED | Posted: 2 January 2024 doi:10.20944/preprints202401.0076.v1

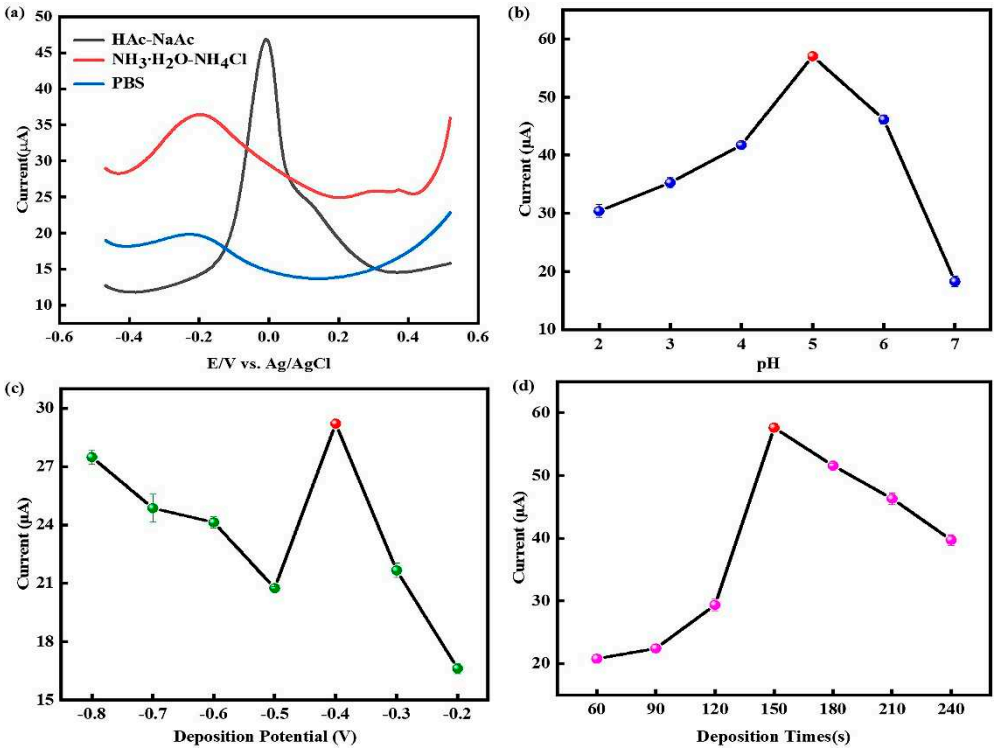

Figure 4. Effect of (a) type of electrolyte solution, (b) pH of selectrolyte solution, (c) deposition potential, and (d) deposition time on the SWSV responses on ZIF-67/MWCNTs/Nafion/GCE.

3.4. Detection of Cu^{2+} by SWSV

The electrodes of different modified materials were analyzed by SWSV in HAc-NaAc solution containing 0.2 μM Cu^{2+}. As shown in the SWSV curve shown in Figure 5a, the stripping peak appearing at approximately -0.1 V is the stripping peak potential of Cu^{2+}. The peak current response of ZIF-67/GCE was three times higher than that of the bare GCE, which was attributed to the good adsorption performance and catalytic activity of ZIF-67. The MWCNTs/GCE showed a higher electrochemical signal but a weaker dissolution peak for Cu^{2+}, reflecting the indispensability of ZIF-67. When the electrode was modified by ZIF-67 and MWCNTs, the response of Cu^{2+} significantly increased, which was attributed to the increase in the number of active site of MWCNTs and the superior conducting ability. When Nafion is added, the sensor performance of the electrode is further improved, which is due to the ability of Nafion to enhance the adsorption capacity of heavy metal ions through electrostatic attraction. Meanwhile, the modification of Nafion can improve the stability of the electrode and effectively prevent the accessories on the electrode surface from falling off. Therefore, ZIF-67/MWCNTs/Nafion was selected as the electrode modification material.

The sensitivity of the sensor was tested by using ZIF-67/MWCNTs/Nafion/GCE as the working electrode under optimized experimental conditions. In the illustration of Figure 5b, it can be found that the peak current increases with increasing Cu^{2+} concentration in the range of 0.2~0.8 μM. Correspondingly, in the calibration curve in Figure 4, the Cu^{2+} concentration is positively correlated with the stripping peak of Cu^{2+}. The linear equation is y=57.5x+2.3152 (R^2=0.9904). The sensitivity of the sensor constructed by ZIF-67/MWCNTs/Nafion to detect Cu^{2+} is 57.5 μA/μM. According to the 3σ/S criterion (where σ is the standard deviation and S is the slope of the calibration graph) [39], the limit of detection (LOD) was calculated to be 15.0 nM. This shows that the electrochemical sensor constructed by ZIF-67, MWCNTs and Nafion has a synergistic effect on the detection of Cu^{2+}, and Cu^{2+} can be effectively reduced and stripped to realize the trace detection of Cu^{2+}.

Preprints (www.preprints.org) | NOT PEER-REVIEWED | Posted: 2 January 2024 doi:10.20944/preprints202401.0076.v1

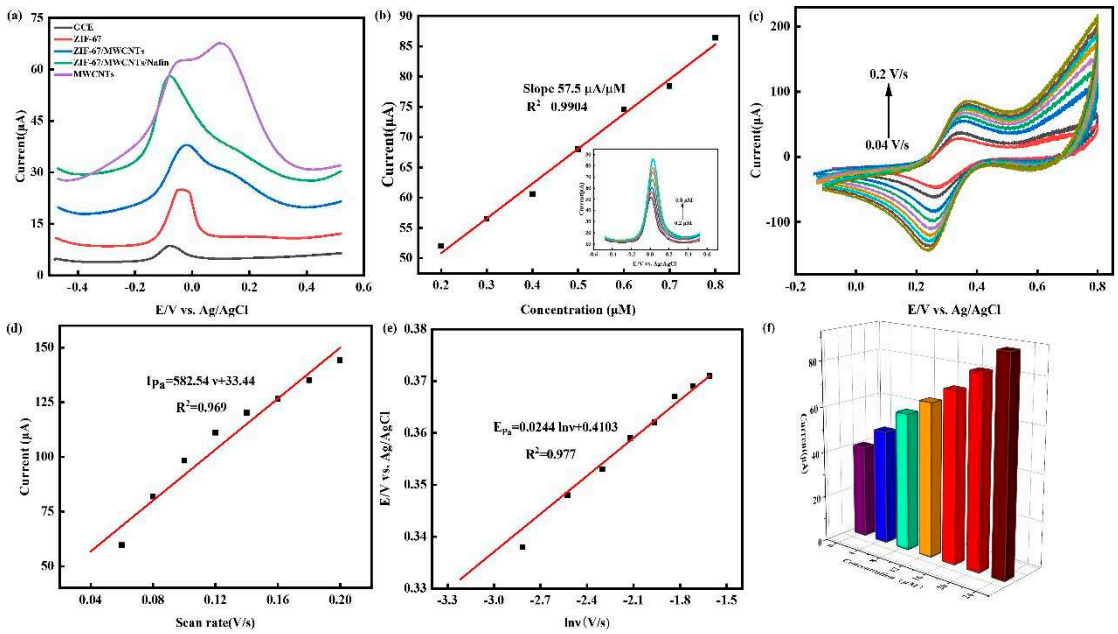

Figure 5. a) SWSV curves of different modified material electrodes: GCE, ZIF-67/GCE, MWCNTs/GCE, ZIF-67/MWCNTs/GCE and ZIF-67/MWCNTs/Nafion/GCE; (b)Linear relationships of ZIF-67/MWCNTs/Nafion/GCE at different concentrations (The illustrations are SWSV curves of ZIF-67/MWCNTs/Nafion/GCE at different concentrations); (c) CV curves of 0.2 μM Cu^{2+} in 0.1 M HAc-NaAc solution with different scanning rates (0.04~0.2 V/s) on ZIF-67/MWCNTs/Nafion/GCE, (d) Linear relationship between oxidation peak current and scanning rate, (e) Linear relationship between oxidation peak potential (E_{pa}) and lnν; (f) Influence of different concentrations Co^{2+} at ZIF-67/MWCNTs/Nafion/GCE.

3.5. Effect of scan rate

To determine the mechanism of electrochemical oxidation of Cu^{2+} by ZIF-67/MWCNTs/Nafion/GCE. The effect of scan rate was investigated using CV. Figure 5c shows the cyclic voltammograms obtained for 0.2 μM Cu^{2+} at different scan rates (0.04-0.2 V/s). From Figure 5d, it can be seen that the oxidation peak current (Ipa) of Cu^{2+} gradually increases with the increase of the scan rate. the I_{pa} of Cu^{2+} is linearly correlated with the scan rate, and the linear equation is: I_{pa}(μA) =582.54 ν+33.44(V/s) (R^2=0.969). From the equation, it can be seen that the current is linearly related to the scan rate. Therefore, the redox behavior of Cu^{2+} on ZIF-67/MWCNTs/Nafion/GCE is a typical adsorption-controlled process [40]. In addition, it can be seen from Figure 5e that the oxidation peak potential (E_{pa}) tends to be positively shifted with the increase of scanning rate, and its linear equation is E_{Pa} = 0.0244 lnν + 0.4103 (R^2=0.977). These results indicate that the electrochemical oxidation process of Cu^{2+} on ZIF-67/MWCNTs/Nafion/GCE is irreversible. The electron transfer number (n) can be obtained according to the Laviron equation [41].

$$E_{pa} = E^{\theta} + \frac{RT}{\alpha nF}\ln\frac{RTK^{\theta}}{\alpha nF} + \frac{RT}{\alpha nF}\ln v$$

where α, n, k^{θ}, and T are the electron transfer coefficient, electron transfer number, electron transfer rate constant, and absolute temperature, respectively. Based on this equation, the value of αn was calculated to be 1.053. Using the recognized value of α of 0.5 for irreversible reactions, the number of electrons involved in the electrochemical oxidation of Cu^{2+} was calculated to be 2.12. This indicates that the electrochemical oxidation of Cu^{2+} on the surface of the sensor based on ZIF-67/MWCNTs/Nafion/GCE is the behavior of the two protons and two electrons involved.

3.6. Effect of Co^{2+} on the detection of Cu^{2+}

Preprints (www.preprints.org) | NOT PEER-REVIEWED | Posted: 2 January 2024 doi:10.20944/preprints202401.0076.v1

A constant deposition potential of -0.4 V was applied to the working electrode. Electrons are transferred from the working electrode to the ZIF-67/MWCNTs /Nafion/GCE interface, where Cu^{2+} obtains electrons and is reduced to Cu. When the forward scanning voltage is applied and the Cu^{2+} stripping peak potential (-0.1V) is reached, the Cu deposited on the electrode is oxidized into Cu^{2+} and returned to the solution. At the same time, electrons return to the surface of the electrode, and the stripping current signal of Cu^{2+} is detected. In this process, ZIF-67 has a good adsorption and catalytic capacity for Cu^{2+}. The addition of MWCNTs and Nafion significantly improves the enrichment degree of Cu^{2+} and the stability of the electrode. For the catalytic ability of ZIF-67, different amounts of Co^{2+} were added to the HAc-NaAc solution to verify the effect on the adsorption of heavy metals. As shown in Figure 5f, the stripping peak of Cu^{2+} is significantly higher than that without the addition of Co^{2+} after the addition of excess Co^{2+} in the HAc-NaAc solution. It can be concluded that Co^{2+} in ZIF-67 plays a catalytic role in the detection of heavy metals [42].

3.7. Research on the repeatability, reproducibility, stability and anti-interference ability of the sensor

In addition to the sensitivity and LOD of the sensor, the repeatability, reproducibility, stability and anti-interference ability of the sensor are also important indicators to detect the performance of the sensor. SWSV tests were performed on ZIF-67/MWCNTs/Nafion/GCE seven consecutive times to verify the repeatability of the electrodes. As shown in Figure 6a, the peak stripping potential of Cu^{2+} was almost consistent in seven tests, and the relative standard deviation (RSD) was 0.49%, which further demonstrated that the electrode had good repeatability. Seven electrodes were used under the same conditions to test the reproducibility of the electrodes. As shown in Figure 6b, the peak stripping potential of the seven electrodes did not deviate significantly, and the RSD was 2.21%, less than 5%, which proved that the sensor had good reproducibility. To test the anti-interference ability of the electrode, 4 μM interfering metal ions such as Zn^{2+}, Co^{2+}, Ba^{2+}, Mn^{2+}, K^{+}, Fe^{2+}, Na^{+} , Mg^{2+}, Cr^{6+}, Fe^{2+}, Hg^{2+}、Cd^{2+} and Pb^{2+} were added to the solution containing 0.2 μM Cu^{2+}. It can be clearly observed from Figure 6c that after the addition of a high concentration of interfering ions, the detection of Cu^{2+} (within 8%) was not affected. This indicates that the sensor has high selectivity. Finally, stability tests were conducted on the original electrode, and the electrode was placed seven days later. As shown in Figure 6d, the peak current seven days later was 95% of the original, indicating that the sensor had good stability.

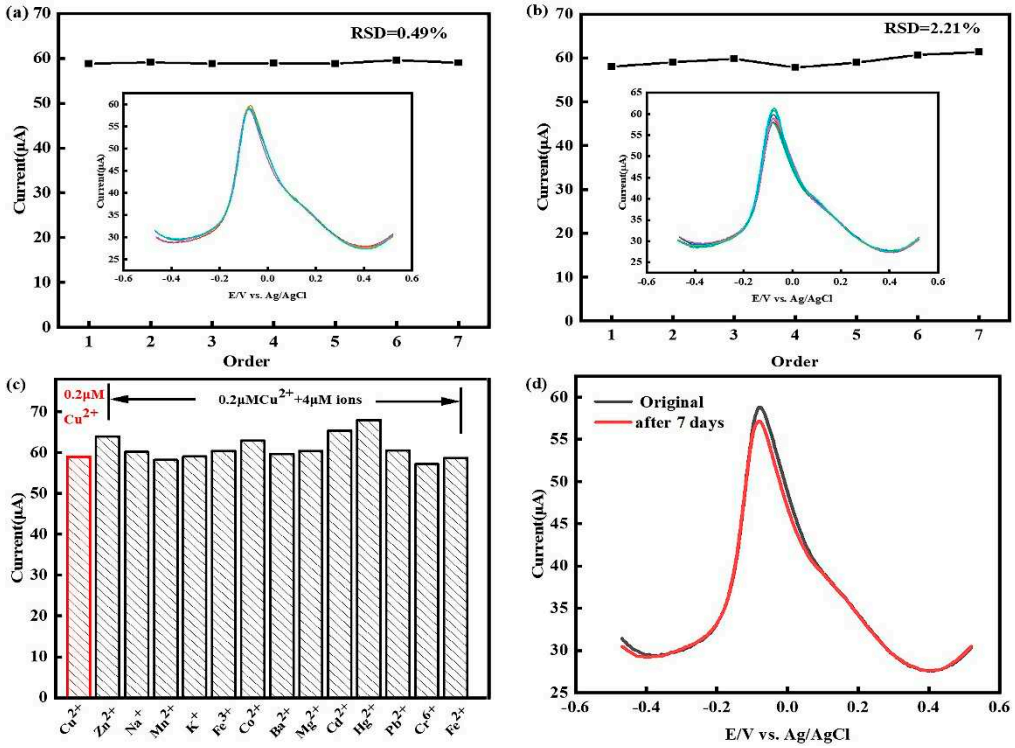

 doi:10.20944/preprints202401.0076.v1

Figure 6. a) Repeatability of ZIF-67/MWCNTs/Nafion/GCE with 7 times of consecutive measurements, (b) Reproducibility of ZIF-67/MWCNTs/Nafion/GCE with 7 times of fabricated sensors, (c)The bar graph for Cu^{2+} peak current intensity of Cu^{2+} (0.2 μM) in 0.1 M HAc-NaAc solution (pH 5.0) in the presence of various metal ions (4.0 μM), (d) The stability of ZIF-67/MWCNTs/Nafion/GCE after 7 days of storage at room temperature.

3.8. Testing of real water samples

The feasibility of ZIF-67/MWCNTs/Nafion/GCE in practical applications was further studied, and SWSV was determined for Cu^{2+} in mineral water and tap water. The results obtained at a ratio of 2:8 between the water sample and HAc-NaAc solution are shown in Table 1. The recovery rate of tap water and mineral water was 98.6%-103%, and the RSD was less than 5%. This indicates that the electrochemical sensor based on ZIF-67/MWCNTs/Nafion can be used to detect Cu^{2+} in actual water samples.

Table 1. Recovery measurements of Cu^{2+} in tap water and mineral water samples using ZIF-67/MWCNTs/Nafion/GCE.

water sample	Added (μM)	Found (μM)	Recovery (%)	RSD (%)
	0.3	0.51	102.0	1.40
	0.5	0.69	98.6	1.02
tap water	0.7	0.93	103.0	2.32
mineral water	0.3	0.49	98.0	1.43
	0.5	0.72	102.9	1.99
	0.7	0.89	99.6	0.08

4. Conclusion

In conclusion, ZIF-67/MWCNTs/Nafion composites were prepared in a simple and environmentally friendly way. ZIF-67/MWCNTs/Nafion/GCE detected the SWSV of Cu^{2+} in the linear range (0.2~0.8 μM), and the LOD was 15.0 nM, which realized the trace detection of Cu^{2+}. Moreover, the sensor showed high sensitivity, selectivity and stability for Cu^{2+}. The applicability of this method is verified by the detection of Cu^{2+} in real water samples, and satisfactory results are obtained. These results indicate that the Cu^{2+} sensor platform based on ZIF-67/MWCNTs/Nafion has great application potential.

Acknowledgments: This work was supported by the Cultivate Scientific Research Excellence Programs of Higher Education Institutions in Shanxi (CSREP2019KJ038) and the Applied Basic Research Youth Fund Program of Science and Technology Department of Shanxi Province (20210302124197).

References

1. Lvova, L. Chemical sensors for heavy metals/toxin detection. Chemosensors, **2020**, 8: 14. [CrossRef]
2. Zhu, S.; Chen, B.; He, M.; Huang, T.; Hu, B. Speciation of mercury in water and fish samples by HPLC-ICP-MS after magnetic solid phase extraction. Talanta. **2017**, 171:213-219. [CrossRef]
3. Guo, Y.; Liu, C.; Ye, R. Advances on water quality detection by uv-vis spectroscopy. Appl. Sci. **2020**, 10:6874. [CrossRef]
4. Chen, S.; Li, Y.; Li, P.; Xiao, X.; Jiang, M.; Li, S.; Zhou, W.; Yang, M.; Huang, X.; Liu, W. Electrochemical spectral methods for trace detection of heavy metals: A review. Trac. Trend. Anal. Chem. **2018**, 106:139-150. [CrossRef]
5. Ding, Q.; Li, C.; Wang, H.; Xu, C.; Kuang, H. Electrochemical detection of heavy metal ions in water. Chem. Commun. **2021**, 57:7215-7231. [CrossRef]
6. Chen, Y.; Bai, X.; Ye, Z. Recent progress in heavy metal ion decontamination based on metal–organic frameworks. Nanomaterials, **2020**, 10:1-23. [CrossRef]
7. Zhu, S.; Yang, Y.; Chen, K.; Su, Z.; Wang, J.; Li, S.; Song, N.; Luo, S.; Xie, A. Novel cubic gravel-like EDAPbCl$_4$@ZIF-67 as electrochemical sensor for the detection of protocatechuic acid. J. Alloy. Compd. **2022** 903:163946. [CrossRef]

8. Wang, G.; Liu, J.; Yue, F.; Shen, Z.; Xu, d.; Fang, H.; Chen, W.; Wang, Z.; Li, P.; Guo, Y.; Snu, X. Dual enzyme electrochemiluminescence sensor based on in situ synthesis of ZIF-67@AgNPs for the detection of IMP in fresh meat. LWT. **2022**, 65:113658. [CrossRef]
9. Hou, Y.; Wang, J.; Liu, S.; Sun, Y.; Dai, Y.; Luo, C.; Wang, X. A novel flower-shaped Ag@ZIF-67 chemiluminescence sensor for sensitive detection of CEA. Talanta. **2023**, 253:123938. [CrossRef]
10. Hussain, Z.; Arif, D.; Sohail, M.; Liaqat, M. A., Khan , M. A., Noor, T. A non-enzymatic electrochemical sensor for glucose detection based on Ag@TiO_2@ Metal-Organic Framework (ZIF-67) nanocomposite. Front. Chem. **2020**, 8:573510. [CrossRef]
11. Fan, J.; Jiang, L.; Lv, H.; Qin, F.; Fan, Y.; Wang, J.; Ikram, M.; Shi, K. ZIF-67/BiOCl nanocomposites for highly efficient detection of NO_2 gas at room temperature. Journali. Mater. Chem. A. **2023**, 11:15370-15379. [CrossRef]
12. Ma, Z.; Yang, B.; Song, Y.; Song Y.; Sun, J. Highly conductive ZIF-67 derived La-doped hollow structure for H_2S detection. Sens. Actuat. B. Chem. **2023**, 379:133139. [CrossRef]
13. Han S, Sun R, Teng F, Wang, Y.; Chu,H.; Zong, W.; Chen, Y.; Sun, Z. A highly selective molecularly imprinted electrochemical sensor with anti-interference based on GO/ZIF-67/AgNPs for the detection of p-cresol in a water environment. Anal. Methods. **2022**, 14:3079-3086. [CrossRef]
14. Liu, X.; Yao, Y.; Ying. Y.; Ping, J. Recent advances in nanomaterial-enabled screen-printed electrochemical sensors for heavy metal detection. Trac. Trend. Anal Chem. 115: 187-202. [CrossRef]
15. Mandal, S.; Natarajan, S.; Mani, P.; Pankajakshan, A. Post-synthetic modification of metal–organic frameworks toward applications. Adv. Funct. Mater. **2021**, 31:2006291. [CrossRef]
16. Sawan, S.; Maalouf, R.; Errachid, A.; Jaffrezic, R. Metal and metal oxide nanoparticles in the voltammetric detection of heavy metals: A review. Trac. Trend. Anal. Chem. **2020**, 131:116014. [CrossRef]
17. Shellaiah, M.; Sun, K. W. Progress in metal-organic frameworks facilitated mercury detection and removal. Chemosensors, **2021**, 9: 101. [CrossRef]
18. Baghayeri, M.; Amiri, A.; Karimabadi, F.; Di Masi, S.; Maleki, B.; Adibian, F.; Pourali, A.; Malitesta, C. Magnetic MWCNTs-dendrimer: A potential modifier for electrochemical evaluation of As (III) ions in real water samples. J. Electroanal. Chem. **2021**, 888:115059. [CrossRef]
19. Filik, H.; Avan, A.A. Neutral red interlinked gold nanoparticles/multiwalled carbon nanotubes modified electrochemical sensor for simultaneous speciation and detection of chromium (VI) and vanadium (V) in water samples. Microchem. J. **2020**, 158:105242. [CrossRef]
20. Nguyen, L. D.; Huynh, T. M.; Nguyen, T. S. V.; Le, D. N.; Baptist, R.; Doan, T. C. D.; Dang C. M. Nafion/platinum modified electrode-on-chip for the electrochemical detection of trace iron in natural water. J Electroanal Chem **2020** 873:114396. [CrossRef]
21. Alexandratos, S. D. From ion exchange resins to polymer-supported reagents: an evolution of critical variables. J. Chem. Technol. Biot. **2018**, 93: 20-27. [CrossRef]
22. Yu, L.; Zhang, Q.; Yang, B.; Xu, Q.; Xu, Q.; Hu, X. Electrochemical sensor construction based on Nafion/calcium lignosulphonate functionalized porous graphene nanocomposite and its application for simultaneous detection of trace Pb^{2+} and Cd^{2+}. Sens. Actuat. B. Chem. **2018**, 259:540-551. [CrossRef]
23. Şahin, F.; Topuz, B.; Kalıpçılar, H. Synthesis of ZIF-7, ZIF-8, ZIF-67 and ZIF-L from recycled mother liquors. Micropor. Mesopor. Mat. **2018**, 261:259-267. [CrossRef]
24. Sezer, N.; Koç, M. Oxidative acid treatment of carbon nanotubes. Surf. Interfaces. **2019**, 14:1-8. [CrossRef]
25. Li, Z.; Guo, Z.; Zhang, T.; Li, Q.; Chen, J.; Ji, W.; Liu, C.; Wei, Y. Fabrication of in situ ZIF-67 grown on alginate hydrogels and its application for enhancing Cu (II) adsorption from aqueous solutions. Colloid. Surface. B. **2021**, 207:112036. [CrossRef]
26. Yu, H.; Kang, J.; Huang, L.; Wang, J.; Wang, X.; Zhao, X.; Du, C. Co/Zn-metal organic frameworks derived functional matrix for highly active amorphous Se stabilization and advanced lithium storage. Rare Metals. **2023**, 42:76-84. [CrossRef]
27. Wang, F.; Zhao, D.; Li, W.; Zhang, H.; Li, B.; Hu, T.; Tan, L. Rod-shaped units based cobalt (II) organic framework as an efficient electrochemical sensor for uric acid detection in serum. Microchem. J. **2023**, 185:108154. [CrossRef]
28. Yang, B.; Shao, M.; Xu, Y.; Du, Y., Yang, H.; Bin, D.; Lu, H. Core-Shell ZIF-8@ZIF-67-Derived Cobalt Nanoparticles In Situ Grown on N-doped Carbon Nanotube Polyhedra for Ultrasensitive Electrochemical Detection of Chloramphenicol. ChemElectroChem. **2022**, 9:e202200438. [CrossRef]
29. Wang, S.; Cao, Y.; Liang, C.; Geng, S.; Guo, H., Liu, Y.; Li, L. Application of ZIF-67 based nitrogen-rich carbon frame with embedded Cu and Co bimetallic particles in QDSSCs. Sol. Energy. **2022**, 237:144-152. [CrossRef]
30. Liu, Z.; Ye, D.; Zhu, X.; Wang, S.; Zou, Y.; Lan, L.; Liao, Q. ZIF-67-derived Co nanoparticles embedded in N-doped porous carbon composite interconnected by MWCNTs as highly efficient ORR electrocatalysts for a flexible direct formate fuel cell. Chem. Eng. J. **2022**, 432:134192. [CrossRef]

31. Nataraj, N.; Chen, T.; Chen, S.; Tseng, T. W.; Bian, Y.; Sun, T.; Jiang, J. Metal-organic framework (ZIF-67) interwoven multiwalled carbon nanotubes as a sensing platform for rapid administration of serotonin. J. Taiwan. Inst. Chem. E. **2021**, 129:299-310.[CrossRef]
32. Shen, H.; He, J.; Shao, X.; Su, Q.; Zhao, D.; Feng, S. Effect of partial substitution of Zn^{2+} with Co^{2+} on catalytic methane combustion performance of $Zn_{1-x}Co_xGa_2O_4$ (X= 0, 0.1, 0.3) microspheres. Solid. State. Sci. **2021**,118:106678. [CrossRef]
33. Yu, Y.; You, S.; Du, J.; Xing, Z.; Dai, Y.; Chen, H.; Zou, J. ZIF-67-derived CoO (tetrahedral Co^{2+})@ Nitrogen-doped porous carbon protected by oxygen vacancies-enriched SnO_2 as highly active catalyst for oxygen reduction and Pt co-catalyst for methanol oxidation. Appl. Catal. B. Environ. **2019**, 259:118043. [CrossRef]
34. Lu, Z.; Zhao, W.; Wu, L.; He, J.; Dai, W.; Zhou, C.; Ye, J. Tunable electrochemical of electrosynthesized layer-by-layer multilayer films based on multi-walled carbon nanotubes and metal-organic framework as high-performance electrochemical sensor for simultaneous determination cadmium and lead. Sens. Actuat. B. Chem. **2021**, 326:128957. [CrossRef]
35. Alimohammady, M.; Jahangiri, M.; Kiani, F.; Tahermansouri, H. Preparation and characterization of functionalized MWCNTs-COOH with 3-amino-5-phenylpyrazole as an adsorbent and optimization study using central composite design. Carbon. Lett. **2019**, 29:1-20. [CrossRef]
36. Heidarzadeh, T.; Nami, N.; Zareyee, D. Application of (MWCNTs)-COOH/CeO_2 hybrid as an efficient catalyst for the synthesis of some nitrogen-containing organic compounds. Inorg. Nano. Met. Chem. **2022**,52:1173-1182. [CrossRef]
37. Zhang. Y.; Yu. H.; Liu, T.; Li, C.; Hao, X.; Lu, Q.; Liang, X.; Liu, F.; Liu, F.; Wang, C.; Yang, C.; Zhu, C.; Lu, G.; Highly sensitive detection of Pb^{2+} and Cu^{2+} based on ZIF-67/MWCNT/Nafion-modified glassy carbon electrode. Anal. Chim. Acta. **2020**, 1124:166-175. [CrossRef]
38. Wen, T.; Wang, L.; Gong, Y. Construction of FeOOH modified CoM_xO_y (M= Mo, W, V) on nickel foam for highly efficient oxygen evolution reaction. Sustain. Energ. Fuels. **2023**, 7: 977-985. [CrossRef]
39. Liu, Z.; Puumala, E.; Chen, A. Sensitive electrochemical detection of Hg (II) via a FeOOH modified nanoporous gold microelectrode. Sens. Actuat. B. Chem. **2019,** 287: 517-525. [CrossRef]
40. Pushpanjali, P. A.; Manjunatha, J. G. Electroanalysis of sodium alizarin sulfonate at surfactant modified carbon nanotube paste electrode: a cyclic voltammetric study. J. Mater. Environ. Sci. **2019**, 10:939-47. [CrossRef]
41. Laviron, E. (1979) General expression of the linear potential sweep voltammogram in the case of diffusionless electrochemical systems. J. Electroanal. Chem. **1979**, 101:19-28. [CrossRef]
42. Hu, H.; Lu, W.; Liu, X.; Meng, F.; Zhu, J. A high-response electrochemical As (III) sensor using Fe_3O_4-rGO nanocomposite materials. Chemosensors, **2021**, 9:150. [CrossRef]